Reprinted from JOURNAL OF THE ELECTROCHEMICAL SOCIETY
Vol. 145, No. 9, September 1998
Printed in U.S.A.

Lithium Insertion into Disordered Carbons Prepared from Organic Polymers

Yongju Jung, Min Chul Suh, Sang Chul Shim, and Juhyoun Kwak

Department of Chemistry, Korea Advanced Institute of Science and Technology, 373-1 Kusong-dong, Yusong-gu, Taejon 305-701, Korea

ABSTRACT

Disordered carbon samples were prepared from four organic polymers: poly[(*Z*)-1-methoxy-4-phenyl-1-buten-3-yne] [poly(MPBEY)], poly(1,4-diphenyl-1-buten-3-yne) [poly(DPBEY)], poly[5-(2-pyridyl)-2,4-pentadiyn-1-ol] [poly(PyPDO)], and poly(2,4-hexadiyn-1,6-diol) (PHDO). Electrochemical lithium insertion into these disordered carbons was studied with discharge/charge tests, cyclic voltammetry, and ^{7}Li nuclear magnetic resonance (NMR) spectroscopy. In the potential range of 0.0 to 2.5 V vs. Li/Li$^+$, all carbons showed discharge/charge curves with a hysteresis effect unlike typical curves for standard lithium insertion/removal processes in pyrolyzed carbons. This hysteresis may be caused by the lithium-oxygen bonding of the organolithium complexes. ^{7}Li NMR spectra showed two kinds of lithium insertion sites in all carbons: a reversible site from which lithium could be removed in the subsequent charge process and an irreversible site where lithium remains intact. The NMR results suggest that the reversible site lithium has ionic nature in all of the fully Li-inserted carbons.

Introduction

Carbon materials have been recognized as suitable anodes for lithium-ion batteries because of their excellent cycling behavior and much better safety than the metallic lithium negative electrode.[1,2] There have been numerous studies on lithium insertion into various kinds of carbons such as natural and synthetic graphites, cokes, carbon blacks, carbon fibers, mesocarbon microbeads (MCMBs), pyrolyzed polymers, etc., to examine the possibility of using these materials as the negative electrode in lithium-ion batteries.[3-8] Lithium intercalation in graphite, in particular, has been most extensively studied.[3,9-11] It is well established that one lithium atom per six carbon atoms can be intercalated into the graphite layer, and LiC_6 is formed as the first-stage compound.[3]

Recently, there has been significant interest in disordered carbons showing much larger capacity than that of graphite (372 mAh/g).[8,12,13] Such disordered carbons are prepared by pyrolysis of organic precursors below 1000°C. Dahn proposed two mechanisms for electrochemical insertion of lithium into this kind of carbon.[13] First, adsorption of lithium on both sides of the surface of single graphene sheets proceeds in disordered carbons made up predominantly of single graphene sheets.[14] Second, lithium atoms can bind on hydrogen-terminated edges of graphene fragments in carbon materials containing a large amount of hydrogen that show large hysteresis.[15,16]

Usually the disordered carbons have been prepared from commercially available organic precursors. The main weakness of this approach is that aromatic condensation proceeds through a very intricate pyrolysis pathway. As a result, it is impossible to understand the microstructure of carbons on the molecular level which is essential to comprehend lithium insertion into carbons. In this study, we report lithium insertion into disordered carbons prepared from specially designed polymers which make it possible to predict the microstructure of carbons, i.e., defect sites formed on edges of graphene sheet, on the molecular level.[17-20] The polymers were prepared by the metathesis polymerization of diacetylenes and enyne derivatives as shown in Scheme I. Electrochemical lithium insertion into the as-prepared carbons was investigated by discharge/charge tests, cyclic voltammetry, and ^{7}Li nuclear magnetic resonance (NMR) spectroscopy to gain insight into the lithium insertion mechanism into disordered carbons.

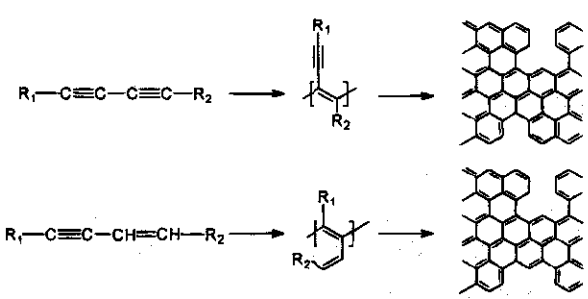

Scheme I. Outline for the preparation of polymers and disordered carbons.

Experimental

Four kinds of organic monomers (Table I) were prepared: (*Z*)-1-methoxy-4-phenyl-1-buten-3-yne (MPBEY), 1,4-diphenyl-1-buten-3-yne (DPBEY), 5-(2-pyridyl)-2,4-pentadiyn-1-ol (PyPDO), and 2,4-hexadiyn-1,6-diol (HDO). These monomers were metathesis polymerized to get poly[(*Z*)-1-methoxy-4-phenyl-1-buten-3-yne] [poly(MPBEY)], poly(1,4-diphenyl-1-buten-3-yne) [poly(DPBEY)], poly[5-(2-pyridyl)-2,4-pentadiyn-1-ol] [poly(PyPDO)], and poly(2,4-hexadiyn-1,6-diol) (PHDO). Disordered carbons were prepared by vacuum pyrolysis of these polymers. The poly(MPBEY) and poly(DPBEY) were pyrolyzed under vacuum at 750°C to get carbons denoted as poly(MPBEY)-750, poly(DPBEY)-750, respectively. The poly(PyPDO) and PHDO were pyrolyzed under vacuum at 800°C to obtain poly(PyPDO)-800, and PHDO-800. The synthesis of organic monomers, the preparation and characterization of the polymers, and the vacuum pyrolysis technique were described in detail elsewhere.[17-20] These samples were ground to a fine carbon powder with sizes less than 100 μm using RETSCH MM 2000 mixer mill. Powder grinding was done in air. The grinding jar (10 mL), balls (10 mm diam) were made of

Table I. Organic monomers used in this study.

(*Z*)-1-methoxy-4-phenyl-1-buten-3-yne (MPBEY)

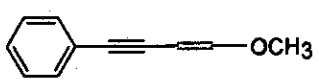

1,4-diphenyl-1-buten-3-yne) (DPBEY)

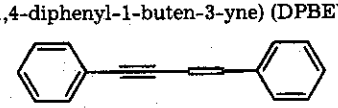

5-(2-pyridyl)-2,4-pentadiyn-1-ol (PyPDO)

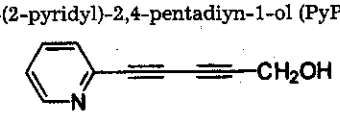

2,4-hexadiyn-1,6-diol (HDO)

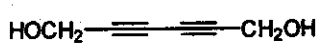

tungsten carbide, Teflon with steel core, respectively. The sample weight and grinding time were about 1 g and 10 min, respectively. X-ray diffractometry (XRD) was carried out using a Rigaku X-ray diffractometer (Rigaku D/MAX-RC 12 kW system) with Cu Kα radiation. The data were collected within a scattering angle (2θ) range from 10 to 100°. Elemental analysis was carried out using an elemental analyzer from Foss Heraeus Analysentechnik Instruments. X-ray photoelectron spectroscopy (XPS) was accomplished with a VG Scientific ESCALAB MK II instruments utilizing Mg Kα X-ray source. In addition, XPS spectra for Lonza KS44 synthetic graphite were measured to compare with those of our samples. The C_{1s} peak of carbon was used as a reference to calibrate the peak position, assuming its binding energy as 285 eV.

The disordered carbons prepared from the organic polymers were mixed with 7 wt % poly(tetrafluoroethylene) binder in isopropyl alcohol. The resulting mixtures were deposited on SUS-EXMET (stainless steel expanded metal grids) and pressed to form electrodes with thicknesses of 300-350 μm. After the carbon electrodes were cured for 3 h at 280°C, they were repressed, dried under vacuum for 24 h at 150°C, and stored in an argon-filled glove box, wherein cells were assembled. Electrochemical measurements were performed in a three-electrode cell with lithium metal as the counter and reference electrodes. The organic electrolyte used was 1.0 M $LiPF_6$ in ethylene carbonate (EC)/diethyl carbonate (DEC) (2/1, vol/vol) solution (battery grade, Mitsubishi Petrochemical Co., Ltd.). The cyclic voltammetry of the carbon electrodes was carried out in the range of 0.0 to 3.0 V vs. Li/Li^+ at scan rates of 1 mV/s. The discharge (inserting lithium) and charge (removing lithium) tests for the carbon electrodes were carried out between 0.0 and 2.5 V vs. Li/Li^+ using a constant current of 24.8 mA/g. At least five cells were tested for each carbon. Fully Li-inserted carbons, and fully Li-removed carbons in the first cycle were prepared by discharging to 0.0 V, and by subsequent charging to 2.5 V after the first discharging to 0.0 V, respectively. The fully Li-inserted carbons and the fully Li-removed carbons were examined by ^7Li NMR spectroscopy (Bruker AM-300; resonance frequency = 116.6 MHz). A solution of 1 M $LiCl/D_2O$ was used as an external standard.

Results and Discussion

Structure and composition of disordered carbons prepared.—Figure 1 shows powder XRD patterns for as-prepared disordered carbons. In all of the carbons, only a few peaks are observed in the XRD patterns, indicating the carbons to be highly disordered.[5] The (002) peak due to the stacking of carbon layers and the (100) peak due to in-plane order are clearly observed at 2θ values near 24 and 45°, respectively. The average crystallite sizes along the *a* axis (L_a) are estimated from the (100) diffraction peak using the Scherrer equation.[21] The carbon samples show (100) peaks with L_a between 26 and 32 Å, which are not significantly different from each other (see Table II). In order to compare the crystallinity between carbon samples, the full width at half-maximum (FWHM) of the (002) peak was utilized because the (002) peak cannot be simply used to measure the average crystallite size along the *c* axis (L_c) for highly disordered carbons.[8] The carbon samples show a very broad (002) peak with FWHM between 7.6 and 10.2 as shown in Table II. These FWHM values are similar to those of epoxy novolak resin (ENR)-derived samples (9.0° in ENR 800), which are known to be made up predominantly of single-layer carbon sheets.[8] In the recent work of Liu et al., the empirical parameter, *R*, which is defined as the ratio of the (002) peak intensity to the background, was reported to be directly related to the fraction of single-layer organized regions in the carbons.[14] All samples in Fig. 1 show *R* values to be about 2 implying that the single-layer fraction is about 35 % as calculated following Ref. 14.

The elemental analysis data are summarized in Table II. All of the carbons show about a 0.2 H/C atomic ratio

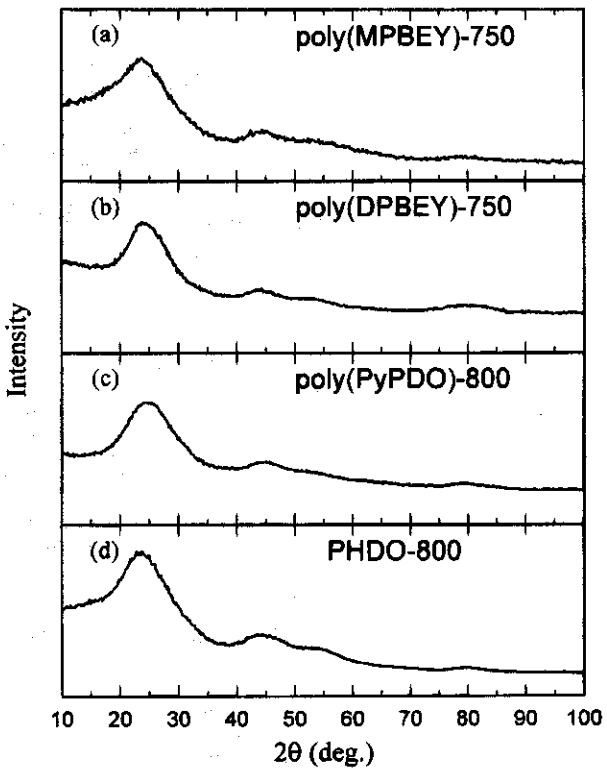

Fig. 1. X-ray diffraction patterns of the prepared carbon samples: (a) poly(MPBEY)-750, (b) poly(DPBEY)-750, (c) poly(PyPDO)-800, and (d) PHDO-800.

which is a little larger compared to those of the ENR 800 sample (0.12) [8] and the PAN-800 sample (0.12) [22] prepared from polyacrylonitrile (PAN). A small amount of nitrogen (N/C = 0.06) is contained in poly(PyPDO)-800 unlike the other carbons.

Figure 2 shows XPS spectra for the C_{1s} of the Lonza KS44, poly(MPBEY)-750, poly(DPBEY)-750, poly(PyPDO)-800, and PHDO-800. It is known that a C_{1s} peak becomes sharper as carbon has more ordered structure.[23] The Lonza KS44 shows the narrowest peak among five carbons as expected. The other carbons, however, have no significant difference from each other. The O_{1s} peak of the Lonza KS44, poly(MPBEY)-750, poly(DPBEY)-750, poly(PyPDO)-800, and PHDO-800 are observed in 532.9, 532.5, 532.9, 532.6, 532.4 eV, respectively, as shown in Fig. 3. The atomic ratio of oxygen to carbon (O/C) calculated from the relative amount of oxygen to carbon (O_{1s}/C_{1s}) of XPS spectra is summarized in Table II. We found that a large amount of oxygen (O/C = 0.12 ~ 0.15) is contained in carbon samples unlike Lonza KS44 graphite (O/C = 0.03). Oxygen exists in oxygen-containing functional groups (i.e., surface oxides) such as carboxyl groups, carboxylic anhydrides, lac-

Table II. Results of elemental analysis and XRD patterns.

Carbon	Atomic ratio H/C[a]	N/C[a]	O/C[b]	(002) FWHM[c] (degree) (±0.5)	L_a(Å)[d] (±2)
poly(MPBEY)-750	0.22	—	0.15	10.2	32
poly(DPBEY)-750	0.19	—	0.12	7.6	31
poly(PyPDO)-800	0.18	0.06	0.14	9.1	30
PHDO-800	0.20	—	0.14	9.9	26
Lonza KS-44	—	—	0.03	0.44	—

[a] H/C and N/C atomic ratio were measured using elemental analyzer.
[b] O/C atomic ratio was calculated from O_{1s} and C_{1s} peaks of XPS spectra.
[c] Full width at half-maximum (FWHM) of (002) peak.
[d] Calculated from the (100) diffraction peak using the Scherrer equation.

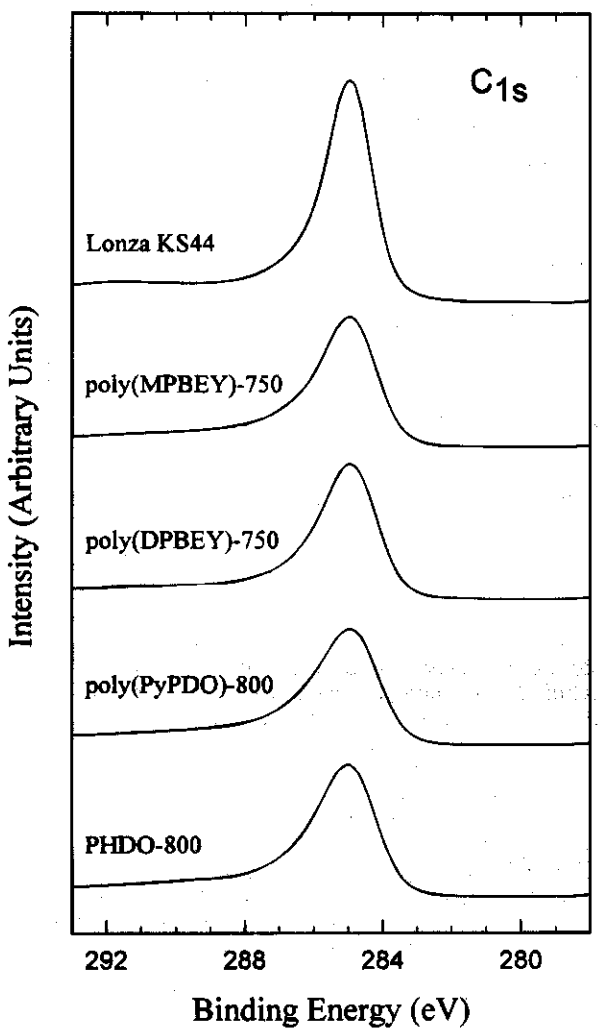

Fig. 2. XPS C_{1s} spectra of Lonza KS44 and the prepared carbons.

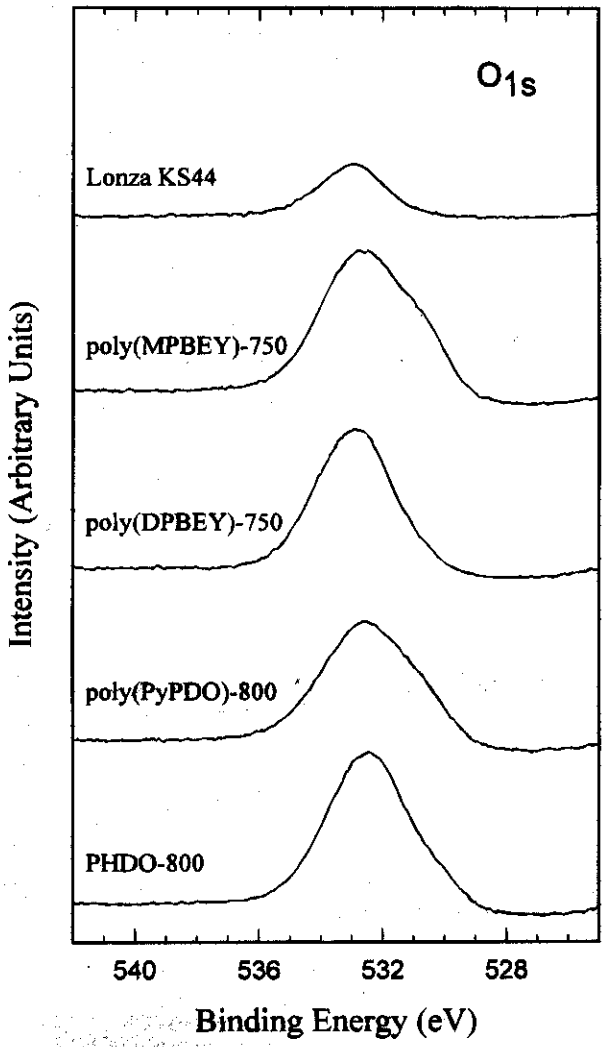

Fig. 3. XPS O_{1s} spectra of Lonza KS44 and the prepared carbons.

tone groups, lactols, hydroxyl groups, ether-type oxygen, and carbonyl groups on the surface of carbon, according to the report of Boehm.[24] It is thought that surface oxides may be formed by chemisorption of moisture, oxygen, and isopropyl alcohol used on making electrodes.

Electrochemical studies on disordered carbons.—Figure 4 shows the discharge and charge curves of the carbon samples during the first two cycles, and the results are summarized in Table III. In the potential range of 0.0 to 2.5 V vs. Li/Li^+, the poly(DPBEY)-750, poly(PyPDO)-800, and PHDO-800 show first charge capacities of 390, 420, and 400 mAh/g, respectively, whereas the poly(MPBEY)-750 shows a much larger capacity (600 mAh/g) than that of graphite (372 mAh/g).

Figure 5 shows the first charge and second discharge curves plotted by reversing the charge curve on the x axis to better compare the voltage profile of the carbon samples. All of the carbons show discharge/charge curves with a large hysteresis effect, unlike typical curves for standard lithium insertion/removal processes in pyrolyzed carbons, where $x \leq 1$ in Li_xC_6, as apparently shown in Fig. 5. This large hysteresis implies that these carbons are not suitable for practical applications. Recently, Xue et al. reported that surface oxides increase both the irreversible and reversible capacities but the reversible capacity due to the surface oxides shows large hysteresis upon oxidation of ENR-derived carbons.[25] It has been well known that lithium forms a very wide range of complexes with amines, ethers, carboxylates, alkoxides, and many other ligands.[26,27] The reaction between lithium and surface functional groups may be classified into two kinds of processes: (*i*) a reversible process in which lithium binds with oxygen-containing functional groups to form organolithium complexes as shown in Scheme II which is conformed with the literature data,[26,27] and (*ii*) an irreversible process. The hysteresis of our samples may be caused by the lithium-oxygen bonding of the organolithium complexes. In the poly(MPBEY)-750, in particular, large capacities with hysteresis are observed and the discharge and charge steps proceed in a higher potential range compared with the other carbons, even though they display similar XRD patterns to each other. Precursor polymers from enynes [poly(MPBEY), poly(DPBEY)] yielded disordered carbons having many more defect sites rather than the most of precursor polymers from diacetylenes [poly(PyPDO), PHDO] because olefin pendant group cannot form honeycomb structures through aromatization.[17-20] It is thought that lithium can reversibly bind with the surface oxides formed on these defect sites leading to larger reversible capacities in poly(MPBEY)-750 compared to other carbons. On the other hand, mesophase carbons can be made from poly(DPBEY) as well as normal carbons, because this polymer has a sterically much more hindered structure compared to poly(MPBEY). It seems that small charge capacity observed in poly(DPBEY)-750 is due to the formation of low molecular weight mesophase carbons which are soluble in electrolyte (in fact, this is observed) and cannot react with lithium reversibly.

The irreversible capacity, observed usually in the first discharge step, is defined as the difference in capacity between the first discharge and the subsequent charge. It is generally accepted that a part of the irreversible capac-

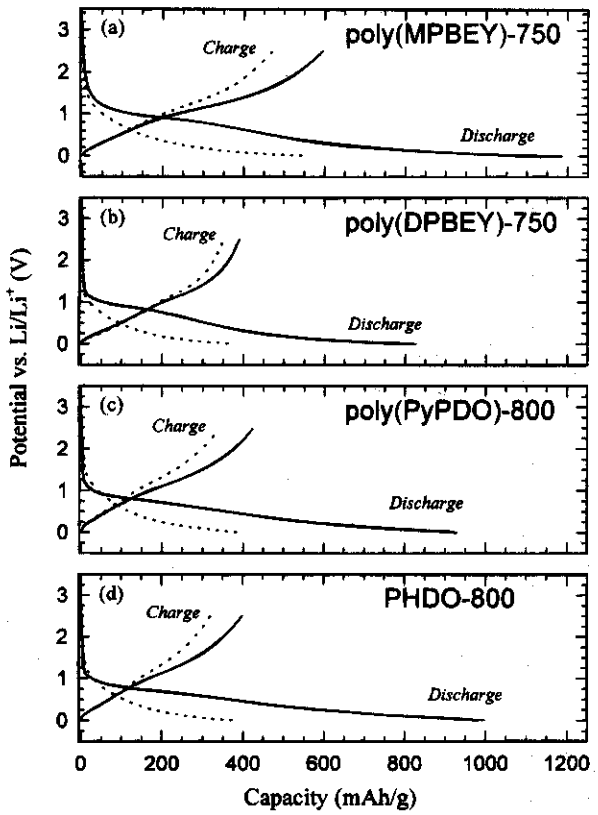

Fig. 4. Discharge/charge curves of the carbon samples: (a) poly(MPBEY)-750, (b) poly(DPBEY)-750, (c) poly(PyPDO)-800, and (d) PHDO-800. The solid and dotted curves correspond to the first and second cycle, respectively.

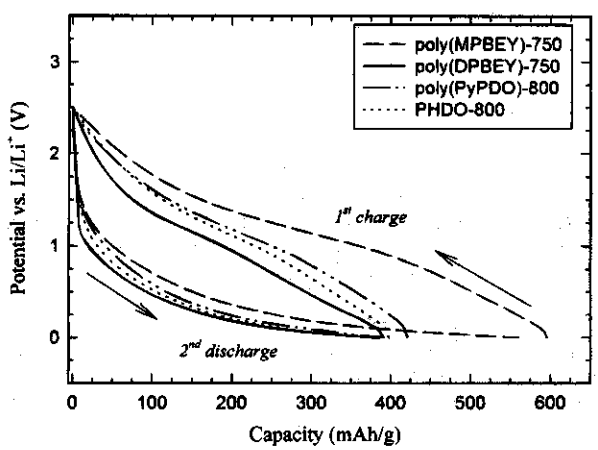

Fig. 5. The first charge and second discharge curves plotted with reversed charge curves.

ity is caused by the formation of a so-called solid electrolyte interface (SEI) on the surface of carbons due to the decomposition of electrolytes.[28] Our samples show very large irreversible capacities (see Table III). This large irreversible capacity makes it impossible to apply these carbons to practical batteries. Xing et al. reported that the irreversible capacity for hard carbons results from two sources: the electrolyte decomposition on nominally clean carbon surface and the reactions with surface functional groups which are formed on carbons exposed to reactive gases.[29] In fact, our samples have many active sites where surface oxides may be formed because they have many defect sites. Some additional irreversible capacity may be caused by the irreversible reaction of lithium with surface functional groups such as −COOH and −OH.[29]

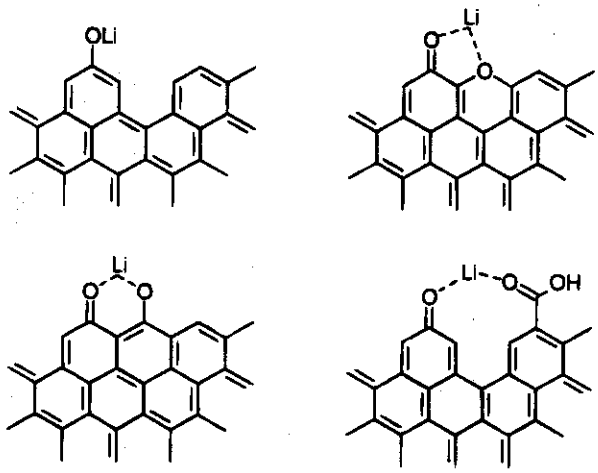

Scheme II. Plausible structures of organolithium complexes.

Figure 6 shows cyclic voltammograms (CV) of the carbon samples. Upon the anodic scan, the charge (lithium removal) capacities are very low in the early cycles and gradually increase during the successive cycles in all of the carbons. The low charge capacities observed in the early cycles illustrate that a large amount of inserted lithium remains in the carbons upon scan reversal. This is consistent with the results observed in the first cycle of our discharge/charge tests. Discharge (lithium insertion) and charge (lithium removal) capacities are calculated for each cycle. The plots of both discharge capacities (Q_{dis}) and charge capacities (Q_{ch}) vs. cycle number are shown in Fig. 7. At the twentieth cycle, poly(MPBEY)-750 and poly (PyPDO)-800 display large charge capacities of about 120 and 110 mAh/g, respectively, while poly(DPBEY)-750 and PHDO-800 show charge capacities of about 55 and 75 mAh/g, respectively. Poly(PyPDO)-800 displays very large capacities during CV tests but shows similar values of charge capacities as those of poly(DPBEY)-750 and PHDO-800 during the discharge/charge tests. These results indicate that the kinetics of lithium insertion/removal in poly(PyPDO)-800 are faster than those of poly(DPBEY)-750 and PHDO-800 probably due to the fast solid-state diffusion of lithium in poly(PyPDO)-800 which consists of small particles of spherical shapes.[19]

^{7}Li NMR spectra of Li-inserted carbons.—To investigate the lithium insertion sites and the chemical state of lithium, ^{7}Li NMR spectra were obtained in both the fully Li-

Table III. Results of the charge/discharge tests for the disordered carbons.

Carbon	Capacity (mAh/g) Discharge 1st	Discharge 2nd	Charge 1st	Charge 2nd	Irreversible capacity[a] (mAh/g)	Cycle efficiency 1st	Cycle efficiency 2nd
poly(MPBEY)-750	1185	560	600	470	585	51	84
poly(DPBEY)-750	825	385	390	350	435	47	91
poly(PyPDO)-800	930	390	420	340	510	45	87
PHDO-800	995	390	400	320	595	40	82

[a] The irreversible capacity is defined as the difference in capacity between the first discharge and the subsequent charge process.

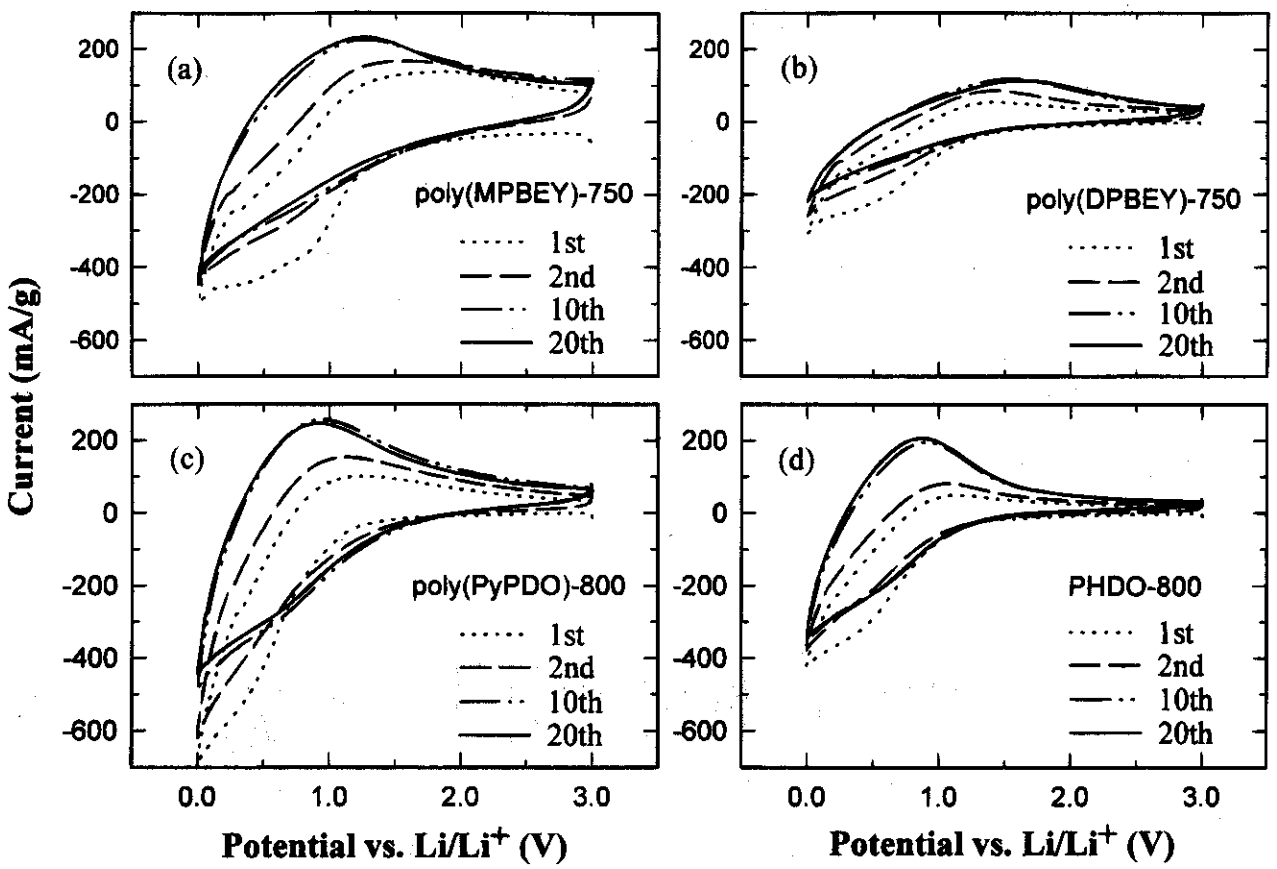

Fig. 6. Cyclic voltammograms of four carbon samples: (a) poly(MPBEY)-750, (b) poly(DPBEY)-750, (c) poly(PyPDO)-800, and (d) PHDO-800.

inserted carbon samples and the fully Li-removed carbon samples after the full lithium insertion in the first cycle (Fig. 8 and 9). The peaks for lithium in the fully Li-inserted poly(MPBEY)-750 (Fig. 8a), poly(DPBEY)-750 (Fig. 8d), poly(PyPDO)-800 (Fig. 9a), and PHDO-800 (Fig. 9d) are observed at about 5.0, 6.5, 4.0, and 6.0 ppm, respectively. The peaks for lithium in the fully Li-removed poly(MPBEY)-750 (Fig. 8b), poly(DPBEY)-750 (Fig. 8e), poly(PyPDO)-800 (Fig. 9b), and PHDO-800 (Fig. 9e) are observed at around −1.0, 1.5, 0.5, and 1.5 ppm, respectively The deconvoluted results for the peaks observed in the fully Li-inserted carbons are shown in Fig. 8c and f, 9c and

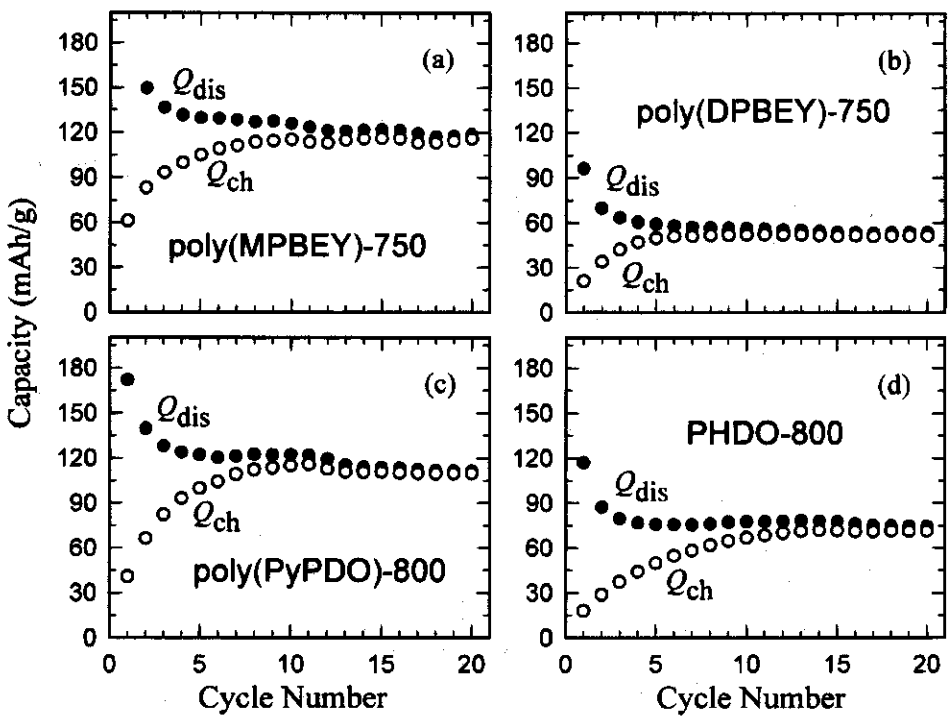

Fig. 7. Plots of both discharge (Q_{dis}) and charge (Q_{ch}) capacities vs. cycle number: (a) poly(MPBEY)-750, (b) poly(DPBEY)-750, (c) poly(PyPDO)-800, and (d) PHDO-800.

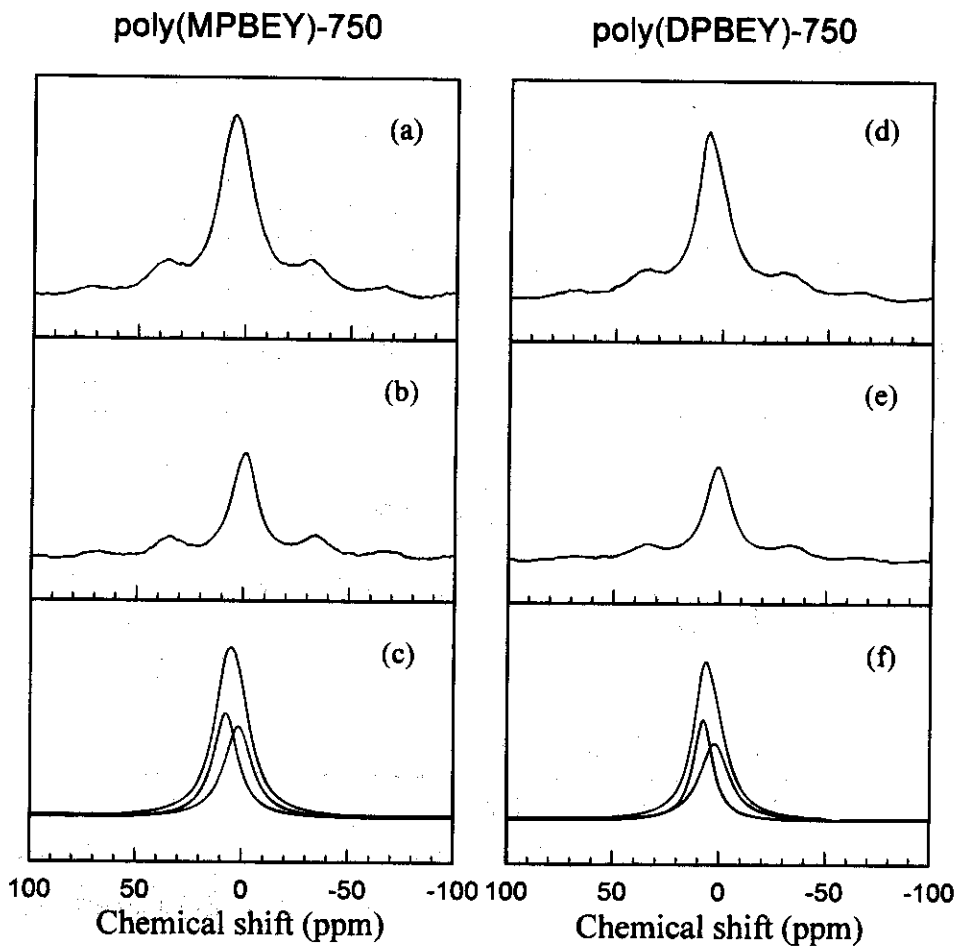

Fig. 8. (a) and (d) are ^{7}Li NMR spectra of fully Li-inserted poly(MPBEY)-750 and poly(DPBEY)-750. (b) and (e) are ^{7}Li NMR spectra of fully Li-removed poly(MPBEY)-750 and poly(DPBEY)-750. (c) and (f) are the deconvoluted results for the main bands in poly(MPBEY)-750 (a) and poly(DPBEY)-750 (d).

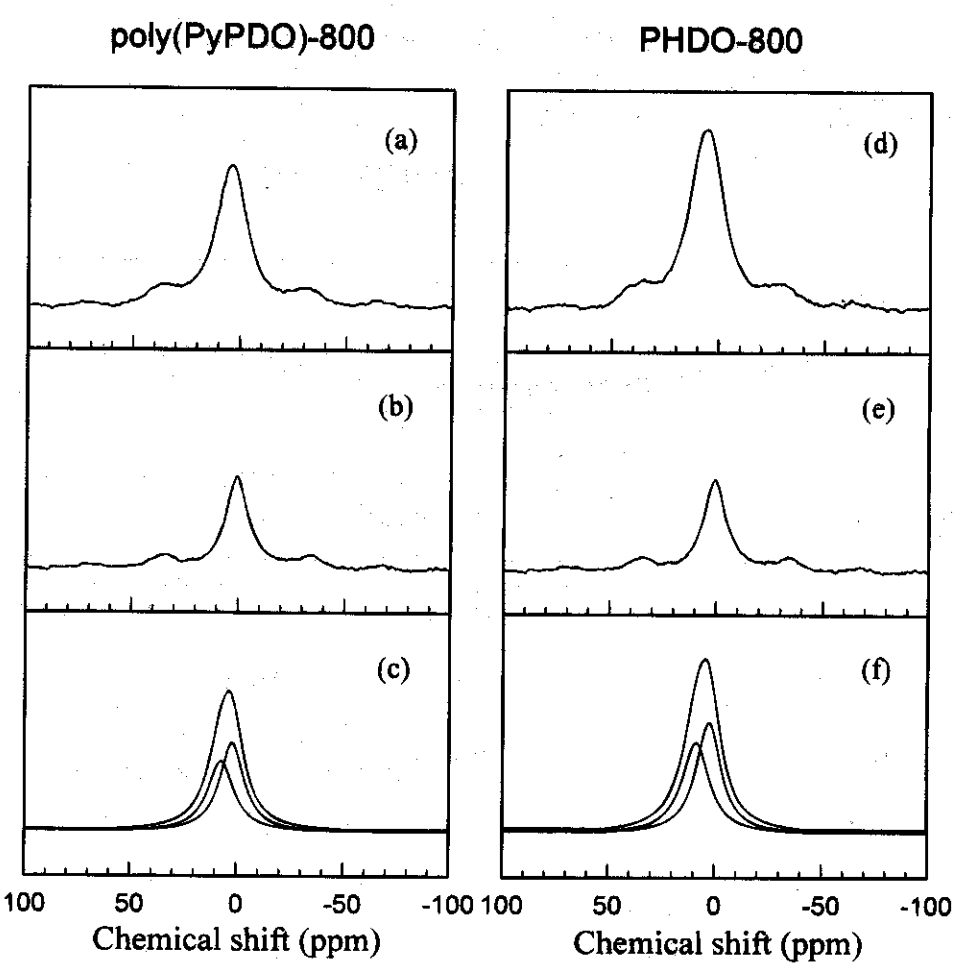

Fig. 9. (a) and (d) are ^{7}Li NMR spectra of fully Li-inserted poly(PyPDO)-800 and PHDO-800. (b) and (e) are ^{7}Li NMR spectra of fully Li-removed poly(PyPDO)-800 and PHDO-800. (c) and (f) are the deconvoluted results for the main bands in poly(PyPDO)-800 (a) and PHDO-800 (d).

Table IV. Results of ^{7}Li NMR spectra on Li-insertion into the disordered carbons.

Carbon	Chemical shift (ppm) (±0.5)	
	Reversible site[a]	Irreversible site[b]
poly(MPBEY)-750	7.5	−1.0
poly(DPBEY)-750	7.5	1.5
poly(PyPDO)-800	7.0	0.5
PHDO-800	9.0	1.5

[a] Obtained by deconvolution of peaks observed in the fully Li-inserted disordered carbons.
[b] Chemical shifts of lithium in the fully Li-removed disordered carbons.

f. The data indicate two kinds of lithium insertion sites: a reversible site from which lithium can be removed during the subsequent charge process and an irreversible site where lithium remains intact. The irreversible site lithium is observed between −1.0 and 1.5 ppm. These values are similar to those of the fully Li-removed PAN-500 sample (ca. 2.0 ppm).[22] It is thought that the irreversible peaks are due to lithium salts formed by irreversible reaction regarding that the quantity of irreversible lithium calculated from NMR results has good correlation with the irreversible capacities listed in Table III. On the other hand, the reversible peaks (7.0 ~ 10 ppm) are observed in the much more upfield region than that of the first-stage graphite intercalation compound fully intercalated with lithium (Li-GIC; ca. 41 ppm) indicating that the reversible-site lithium exists in almost completely ionized state (see Table IV).[30,31] This indicates that the high capacity observed in poly(MPBEY)-750 can be interpreted with neither Mabuchi et al.'s cavity mechanism[2] nor Sato et al.'s mechanism[32] where lithium occupies nearest-neighbor sites between every pair of graphene sheets, both of which were proposed to explain both the high capacity and the large hysteresis which are generally observed in carbons having much hydrogen content, as well described by Tatsumi et al.[30] It seems, however, that the formation of organolithium complexes suggested in the previous section is more probable considering the chemical shift of the reversible peak.

Conclusions

Disordered carbons made from specific organic polymers show very broad (002) peaks with FWHM between 7.6 and 10.2° which are similar to that of an ENR 800 sample (9.0°) made up predominantly of single-layer carbon sheets. XPS spectra show that a large amount of oxygen (O/C = 0.12 ~ 0.15) is contained in all carbon samples unlike Lonza KS44 graphtite (O/C = 0.03). In the potential range of 0.0 to 2.5 V vs. Li/Li$^+$, poly(DPBEY)-750, poly(PyPDO)-800, and PHDO-800 display first charge capacities of 390, 420, and 400 mAh/g, respectively, whereas poly(MPBEY)-750 shows a much larger capacity (600 mAh/g) than graphite (372 mAh/g). All of the carbons show large hysteresis which may be caused by the lithium-oxygen bonding of the organolithium complexes. In addition, these carbons show large irreversible capacity. Unfortunately, these poor electrochemical characteristics make it impossible to apply the carbon materials to practical batteries. ^{7}Li NMR spectra show two kinds of lithium insertion sites in all the carbons: a reversible site from which lithium could be removed in the subsequent charge process and an irreversible site where lithium remains intact. The reversible peaks (7.0 ~ 10 ppm) in all the fully Li-inserted carbon samples are observed in the much more upfield region than that of the first-stage Li-GIC (ca. 41 ppm) providing insight into the ionic nature of the reversible-site lithium.

Acknowledgments

This work was supported by the Samsung Display Devices Co., Ltd., and the Korea Research Institute of Standards and Science.

Manuscript submitted February 9, 1998; revised manuscript received April 24, 1998.

Korea Advanced Institute of Science and Technology assisted in meeting the publication costs of this article.

REFERENCES

1. K. Tatsumi, K. Zaghib, Y. Sawada, H. Abe, and T. Ohsaki, *J. Electrochem. Soc.*, **142,** 1090 (1995).
2. A. Mabuchi, K. Tokumitsu, H. Fujimoto, and T. Kasuh, *J. Electrochem. Soc.*, **142,** 1041 (1995).
3. T. Ohzuku, Y. Iwakoshi, and K.Sawai, *J. Electrochem. Soc.*, **140,** 2490 (1993).
4. M. Jean, A. Tranchant, and R. Messina, *J. Electrochem. Soc.*, **143,** 391 (1996).
5. J. R. Dahn, A. K. Sleigh, H. Shi, J. N. Reimers, Q. Zhong, and B. M. Way, *Electrochim. Acta,* **38,** 1179 (1993).
6. M. W. Verbrugge and B. J. Koch, *J. Electrochem. Soc.,* **143,** 24 (1996).
7. A. Mabuchi, H. Fujimoto, K. Tokumitsu, and T. Kasuh, *J. Electrochem. Soc.*, **142,** 3049 (1995).
8. T. Zheng, Y. Liu, E. W. Fuller, S. Tseng, U. von Sacken, and J. R. Dahn, *J. Electrochem. Soc.*, **142,** 2581 (1995).
9. K. Tatsumi, N. Iwashita, H. Sakaede, H. Shioyama, S. Higuchi, A. Mabuchi, and H. Fujimoto, *J. Electrochem. Soc.*, **142,** 716 (1995).
10. J. R. Dahn, R. Fong, and M. J. Spoon, *Phys. Rev. B,* **42,** 6424 (1990).
11. J. R. Dahn, *Phys. Rev. B,* **44,** 9170 (1991).
12. (a) S. Yata, H. Kinoshita, M. Komori, N. Ando, T. Kashiwamura, T. Harada, K. Tanaka, and T. Yamabe, *Synth. Met.*, **62,** 153 (1994); (b) S. Yata, Y. Hato, H. Kinoshita, N. Ando, A. Anekawa, T. Hashimoto, M. Yamaguchi, K. Tanaka, and T. Yamabe, *Synth. Met.*, **73,** 273 (1995).
13. J. R. Dahn, T. Zheng, Y. Liu, and J. S. Xue, *Science,* **270,** 590 (1995).
14. Y. Liu, J. S. Xue, T. Zheng, and J. R. Dahn, *Carbon,* **34,** 193 (1996).
15. T. Zheng, J. S. Xue, and J. R. Dahn, *Chem. Mater.,* **8,** 389 (1996).
16. T. Zheng, W. R. McKinnon, and J. R. Dahn, *J. Electrochem. Soc.*, **143,** 2137 (1996).
17. M. C. Suh and S. C. Shim, *Macromolecules,* **28,** 8707 (1995).
18. S. C. Shim, M. C. Suh, and D. S. Kim, *J. Polym. Sci., Part A: Polym. Chem.*, **34,** 3131 (1996).
19. M. C. Suh and S. C. Shim, *Chem. Mater.,* **9,** 192 (1997).
20. H. J. Lee and S. C. Shim, *J. Polym. Sci., Part A: Polym. Chem.*, **32,** 2437 (1994).
21. B. E. Warren, *Phy. Rev.*, **59,** 693 (1941).
22. Y. Jung, M. C. Suh, H. Lee, M. Kim, S.-I. Lee, S. C. Shim, and J. Kwak, *J. Electrochem. Soc.*, **144,** 4279 (1997).
23. T. Takahagi and A. Ishitani, *Carbon,* **26,** 389 (1988).
24. H. P. Boehm, *Carbon,* **32,** 759 (1994).
25. J. S. Xue and J. R. Dahn, *J. Electrochem. Soc.*, **142,** 3668 (1995).
26. (a) F. A. Cotton and G. Wilkinson, *Advanced Inorganic Chemistry,* Chap. 4, John Wiley & Sons, Inc., New York (1988); (b) M. A. Beswick and D. S. Wright, in *Comprehensive Organometallic Chemistry II,* Vol. 1, C. E. Housecroft, Editor, Chap. 1, Pergamon Press Inc., New York (1995).
27. D. Seebach, *Angew. Chem. Int. Ed. Engl.*, **27,** 1624 (1988).
28. R. Fong, U. von Sacken, and J. R. Dahn, *J. Electrochem. Soc.*, **137,** 2009 (1990).
29. W. Xing and J. R. Dahn, *J. Electrochem. Soc.*, **144,** 1195 (1997).
30. K. Tatsumi, T. Akai, T. Imamura, K. Zaghib, N. Iwashita, S. Higuchi, and Y. Sawada, *J. Electrochem. Soc.*, **143,** 1923 (1996).
31. W. Müller-Warmuth, in *Progress in Intercalation Research,* W. Müller-Warmuth and R. Schöllhorn, Editors, p. 339, Kluwer Academic Publishers, Norwell, MA (1994).
32. K. Sato, M. Noguchi, A. Demachi, N. Oki, and M. Endo, *Science,* **264,** 556 (1994).